Electronic Supplementary Information

Spatiotemporal control of kinesin motor protein by photoswitches enabling selective single microtubule regulations

K. R. Sunil Kumar, Ammathnadu S. Amrutha and Nobuyuki Tamaoki*

HPLC analysis on the conversion ratio from *E* to *Z* and *Z* to *E forms* of Azo-peptide

The photo conversion ratio from *trans (E)* to *cis (Z)* and *cis* to *trans* of the azo unit in Azo-peptide upon irradiation with 365-nm light and 488- or 510-nm light was measured with Shimadzu reversed-phase (RP) HPLC system. Conditions of the RP-HPLC analysis; Column-5C_{18}-MS-II, 4.6×250 mm (Nacalai Tesque, Inc.); Eluent - CH_3CN/H_2O containing 0.1% TFA; Solvent gradient - 20 to 45% for 1 h; Flow rate – 1 ml min^{-1} at room temperature (25 ^{0}C). Injection volume - 20 µl was used to analyze the ratio of each isomer and the isosbestic point in this eluent condition (305-nm) was used as the monitoring wavelength.

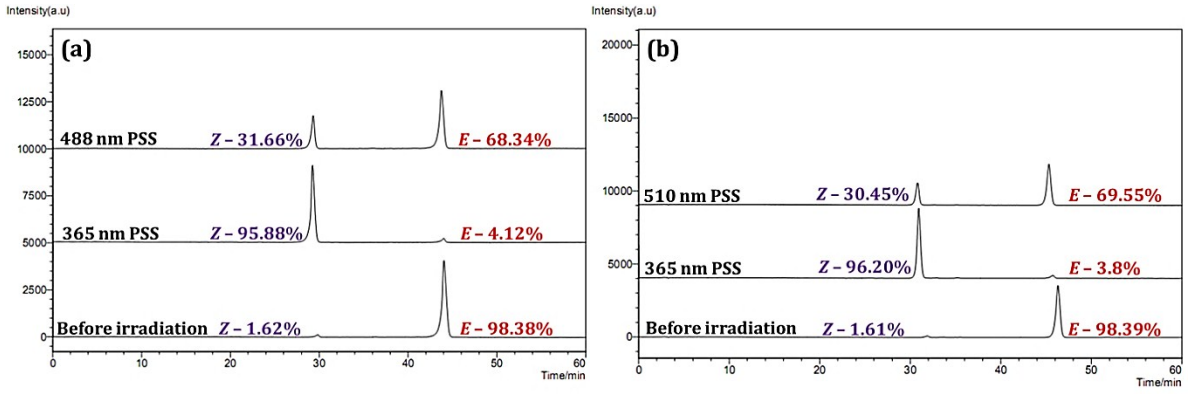

Fig. S1 (a) and (b) HPLC chromatograms show the *Z* and *E* isomer ratio of Azo-peptide at before irradiation, after 365-nm light irradiation up to photo stationary state (PSS) and after 488- or 510-nm light irradiation up to PSS respectively.

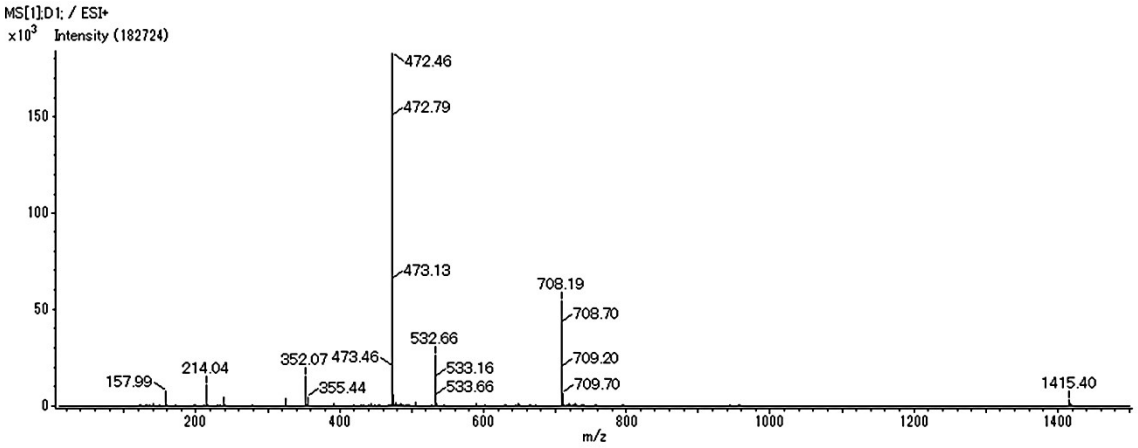

Fig. S2 ESI mass spectrum of Azo-peptide: *m/z* = 1415.40 $[M+H]^+$ (calcd. 1415.75)

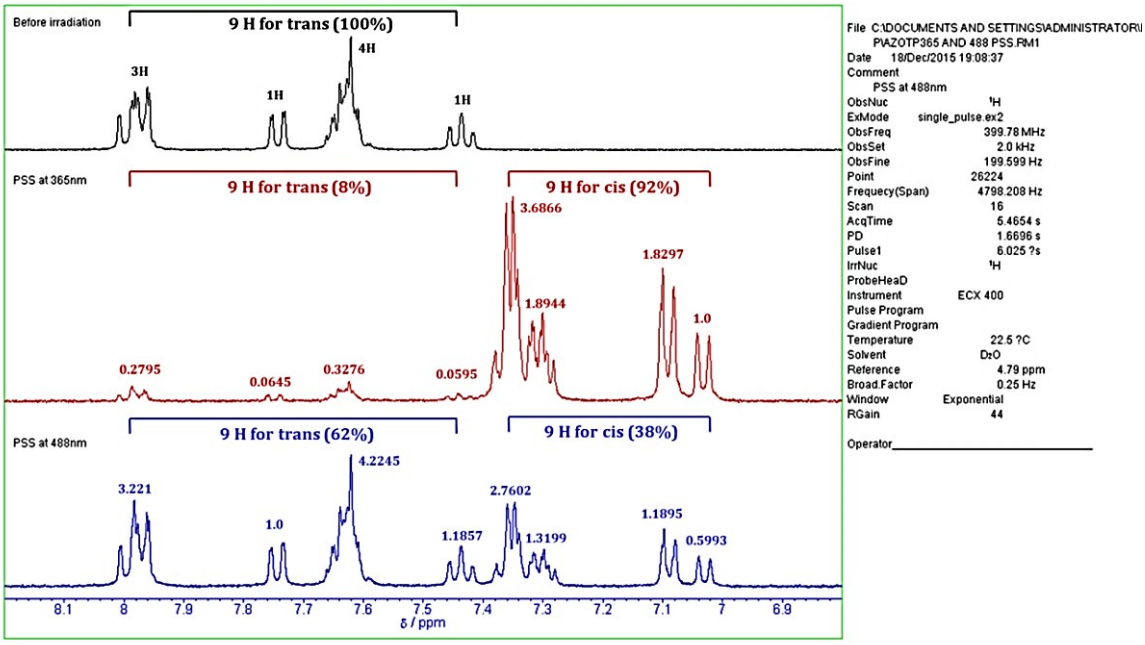

Fig. S3 NMR spectrum shows the *Z* and *E* isomer ratio of AzoTP at before irradiation, after 365-nm light irradiation up to PSS and after 488-nm light irradiation up to PSS respectively.

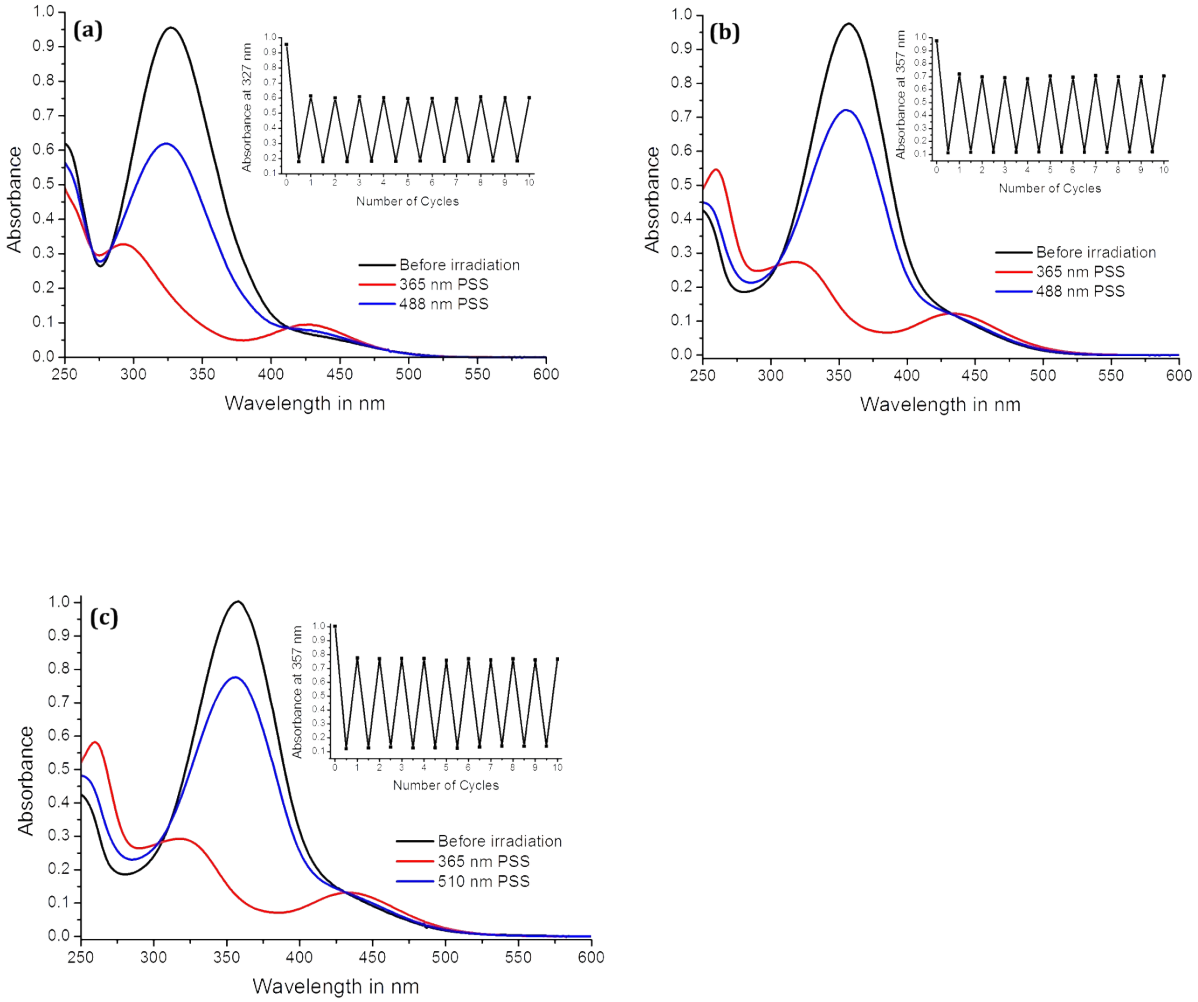

Fig. S4 UV-visible absorption spectra of AzoTP (a) and Azo-peptide (b and c) in BRB-80 buffer solution at 25 ^{0}C; before photo-irradiation (Black line), PSS at 365-nm light irradiation (Red line), PSS at 488- or 510-nm light irradiation (Blue line). The inset shows the absorbance changes (a) at 327-nm after alternating irradiation with 365- and 488-nm light for 10 cycles, (b and c) at 357-nm after alternating irradiation with 365-nm and 488- or 510-nm light for 10 cycles.

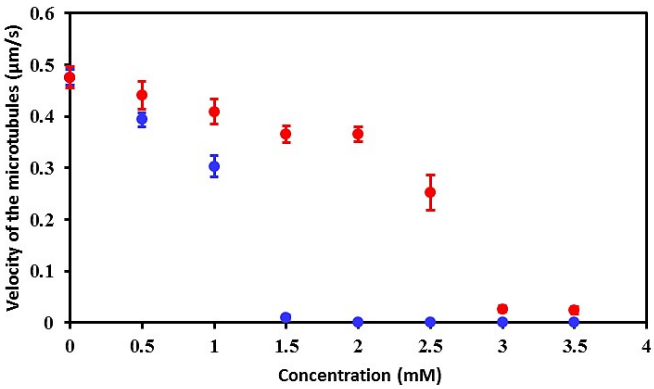

Fig. S5 Gliding velocities of microtubules plotted with respect to the concentration of Azo-peptide at 1.0 mM ATP concentration. Blue circles: gliding velocity of microtubules in non-irradiated state; Red circles: gliding velocity after 365-nm light irradiation up to PSS; Error bars represent the standard deviation for 10 microtubules.

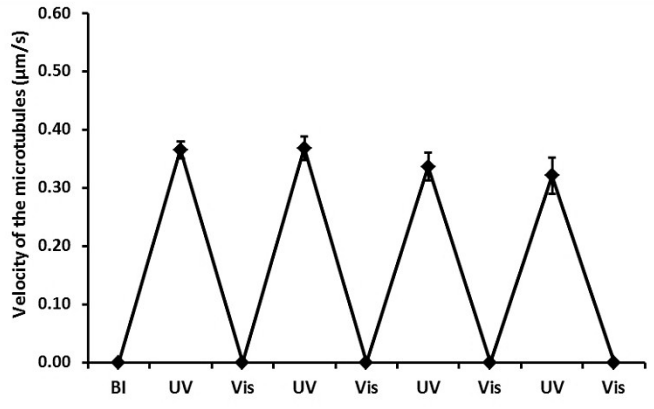

Fig. S6 Repeatability of the photo-controllable change in the gliding velocity of microtubules in presence of Azo-peptide (2.0 mM) upon alternating irradiation with UV and visible lights (BI: Before irradiation, UV: after 365 nm light irradiation for 20 s, Vis: after 510-nm light irradiation for 40 s). Error bars represent the standard deviation for 10 microtubules.

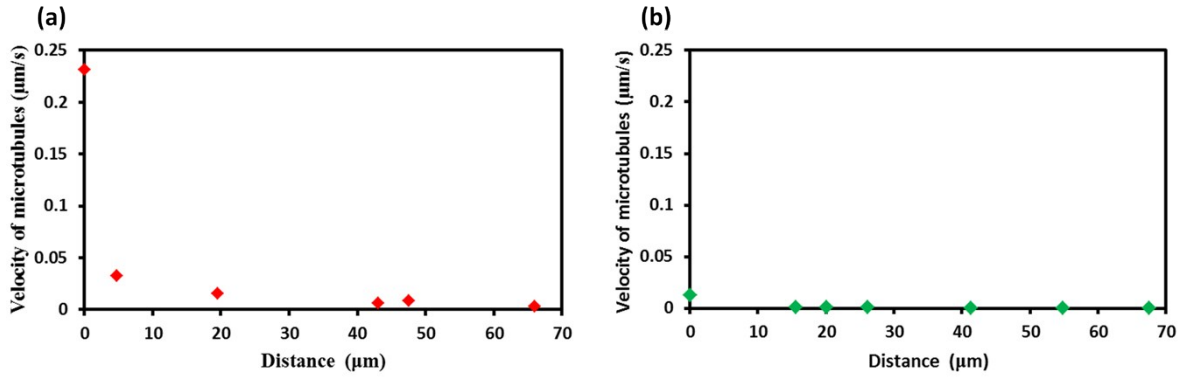

Fig. S7 Activation profile shows the velocity of microtubules at a distance away from the local light illumination area (365 nm) while irradiating entire area with 510 nm in the presence of Azo-peptide [(a) 2.0 mM & (b) 2.5 mM] and ATP (1.0 mM).

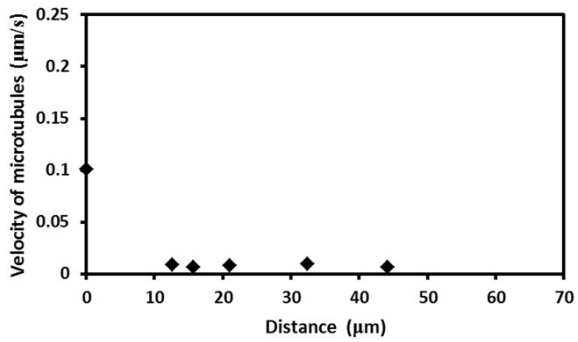

Fig. S8 Activation profile shows the velocity of microtubules at a distance away from the local light illumination area (488 nm) while irradiating entire area with 365 nm in the presence of AzoTP (0.5 mM).

Fluorescence Microscopy Videos (AVI)

Movie S1

This video demonstrates the concentration and dispersion of the fluorescently labeled microtubules in the presence of Azo-peptide (2.5 mM) and ATP (1.0 mM). A local irradiation with 488-nm light covering the area of 18 μm in diameter and keeping entire imaging area under 365-nm light concentrated the microtubules in that area. Upon removal of the 488-nm light irradiation dispersed the microtubules. This was repeated for two times at different positions. However, microtubules were slightly aggregated with each other in the inhibited state (0-30s) due to the high concentration of microtubules (1.5 μM, MTs calculated as tubulin dimer) used. Therefore intense bright images were seen for the aggregated state of the microtubules during first 30 s and they get separated in to single microtubule filaments after 365-nm light irradiation.

Movie S2

This video demonstrates the selective transportation of a single microtubule in the presence of AzoTP (0.5 mM). The selected microtubule was driven by locally irradiating it with 488-nm light covering the area of 5 μm in diameter and keeping entire imaging area under irradiation with 365-nm. Further it was translocated by progressively changing the position of 488-nm light irradiation.

Movie S3

This video demonstrates the selective transportation of a single microtubule in the presence of Azo-peptide (2.0 mM) and ATP (1.0 mM). The selected microtubule was driven by locally irradiating it with 365-nm light covering the area of 5 μm in diameter and keeping entire imaging area under irradiation with 510-nm. Further it was translocated by progressively changing the position of 365-nm light irradiation.

Movie S4

This video demonstrates the bending and breaking of a single microtubule in the presence of Azo-peptide (2.0 mM) and ATP (1.0 mM). We first irradiated the leading end of the selected microtubule locally by 365-nm light covering the area of 5 μm in diameter at the front while keeping entire imaging area under irradiation with 510-nm for 0-23s, which allowed it to move in the forward motion. The selected microtubule was then locally irradiated with 365-nm light covering the area of 5 μm in diameter at the trailing end while keeping entire imaging area under irradiation with 510-nm. At that condition the microtubule started to bend, on its way of bending we changed the position of 365-nm light irradiation towards its leading end to drive forward and avoid further bending. Again, by sufficiently irradiating 365-nm light at the trailing end makes the microtubule to bend and then broken. Further, we confirmed the breaking of the microtubule by irradiating 365-nm light at the leading end which makes the microtubule to move forward and eventually broken parts get separated.